Strong contribution of autumn phenology to changes in satellite-derived growing season length estimates across Europe (1982–2011)

IRENE GARONNA[1], ROGIER DE JONG[1], ALLARD J.W. DE WIT[2], CASPAR A. MÜCHER[2], BERNHARD SCHMID[3] and MICHAEL E. SCHAEPMAN[1]

[1]*Remote Sensing Laboratories, Department of Geography, University of Zurich, Winterthurerstr. 190, 8057 Zurich, Switzerland,* [2]*Earth Observation and Environmental Informatics, Alterra, Wageningen University and Research Centre, P.O. Box 47, Wageningen NL-6700 AA, The Netherlands,* [3]*Institute of Evolutionary Biology and Environmental Studies, University of Zurich, Winterthurerstrasse 190, Zurich 8057, Switzerland*

Abstract

Land Surface Phenology (LSP) is the most direct representation of intra-annual dynamics of vegetated land surfaces as observed from satellite imagery. LSP plays a key role in characterizing land-surface fluxes, and is central to accurately parameterizing terrestrial biosphere–atmosphere interactions, as well as climate models. In this article, we present an evaluation of Pan-European LSP and its changes over the past 30 years, using the longest continuous record of Normalized Difference Vegetation Index (NDVI) available to date in combination with a landscape-based aggregation scheme. We used indicators of Start-Of-Season, End-Of-Season and Growing Season Length (SOS, EOS and GSL, respectively) for the period 1982–2011 to test for temporal trends in activity of terrestrial vegetation and their spatial distribution. We aggregated pixels into ecologically representative spatial units using the European Landscape Classification (LANMAP) and assessed the relative contribution of spring and autumn phenology. GSL increased significantly by 18–24 days decade^{-1} over 18–30% of the land area of Europe, depending on methodology. This trend varied extensively within and between climatic zones and landscape classes. The areas of greatest growing-season lengthening were the Continental and Boreal zones, with hotspots concentrated in southern Fennoscandia, Western Russia and pockets of continental Europe. For the Atlantic and Steppic zones, we found an average shortening of the growing season with hotspots in Western France, the Po valley, and around the Caspian Sea. In many zones, changes in the NDVI-derived end-of-season contributed more to the GSL trend than changes in spring green-up, resulting in asymmetric trends. This underlines the importance of investigating senescence and its underlying processes more closely as a driver of LSP and global change.

Keywords: asymmetric trends, GIMMS, growing season length, land surface phenology, spring vs. autumn phenology, vegetation activity

Received 9 February 2014 and accepted 24 March 2014

Introduction

As anthropogenic pressure on ecosystems is increasingly documented, so is the understanding that its impact is likely to intensify over the coming years (IPCC, 2007; Running, 2012; IPCC, 2013; Rockström *et al.*, 2009). Monitoring vegetation dynamics constitutes a crucial effort for environmental management (Zhou *et al.*, 2001; Reed *et al.*, 2003), and the advances in quality and availability of remote sensing products have proven very fruitful in observing vegetation activity at various scales (e.g., Zhou *et al.*, 2001; Zhang *et al.*, 2003; Running *et al.*, 2004; Turner Ii *et al.*, 2007; Zeng *et al.*, 2013). The Normalized Difference Vegetation Index (NDVI) (Rouse *et al.*, 1974; Tucker, 1979) is the most commonly used

proximate indicator for vegetation activity. It has been used among other purposes to describe seasonal dynamics of vegetation activity (Reed *et al.*, 1994; Julien & Sobrino, 2009) and for assessing interannual trends in these seasonal dynamics, in particular greening and browning trends at various scales (Myneni *et al.*, 1997; Zhou *et al.*, 2001; de Jong *et al.*, 2011).

In the field of Land Surface Phenology (LSP), remote sensing methods are used to study seasonal patterns of vegetated land surfaces (de Beurs & Henebry, 2005; Friedl *et al.*, 2006; Julien & Sobrino, 2009). In contrast with plant phenology, LSP does not aim to describe the physiological cycle of individual plants, but rather to assess vegetation activity over the growing season at the ecosystem level (Stöckli & Vidale, 2004). LSP provides key variables in terrestrial biosphere and climate change models, because green vegetation cover

Correspondence: Irene Garonna, tel. +41-44-6355215, fax +41-44-6356846, e-mail: irene.garonna@geo.uzh.ch

regulates land surface fluxes through albedo, CO_2 assimilation and evapotranspiration (Arora & Boer, 2005; Richardson *et al.*, 2012, 2013). LSP has therefore been proposed as an 'essential biodiversity variable' to be included in monitoring programmes worldwide (Pereira *et al.*, 2013). Furthermore, vegetation seasonality can be used as an important habitat descriptor (Coops *et al.*, 2013).

The fact that Europe is undergoing major environmental change is widely recognized (Menzel & Fabian, 1999; Metzger *et al.*, 2008; EEA, 2012; IPCC, 2013). There is therefore a need to provide integrative assessments of the state and trends shaping the European environment (Hazeu *et al.*, 2011). However, the heterogeneity of ecologically meaningful areas within this region makes it difficult to understand the impact and vulnerability of this region to global climate change (Metzger *et al.*, 2006). Europe's climatic spectrum allows it to encompass a considerable variety of biomes (Meeus, 1995; Bailey & Ropes, 1998; Mücher *et al.*, 2010). Also, the long history of human presence and different types of land-use management helped to shape Europe's complex landscape and vegetation mosaic (Meeus, 1995), which in turn may significant feedback on regional climatic change (Foley *et al.*, 2003). Aggregating pixels of the terrestrial surface into relatively homogeneous vegetation types facilitates the understanding of changes in such a complex region and provides the basis for assessment and monitoring programs at the European scale (Metzger *et al.*, 2005; Mücher *et al.*, 2010).

As one of various environmental classification methods, the European Landscape Classification [LANMAP; (Mücher *et al.*, 2010)] uses a systematic, quantitative and objective approach to incorporate land cover/land use, climate, geomorphology and soil characteristics in a single map (Hazeu *et al.*, 2011). Thus, LANMAP constitutes a more complete categorization of the European environment than would a land cover/land use classification alone. Landscapes reflect the combination of abiotic, biotic and anthropogenic processes that are needed for the analysis of environmental and ecological data at the European scale (Mücher *et al.*, 2010).

In this article, we evaluate NDVI-derived growing season temporal trends and their spatial pattern across all of Europe over the past 30 years, using a landscape-based aggregation scheme. Various previous studies have reported shifts in European growing seasons both from field (Menzel, 2000; Ahas *et al.*, 2002; Menzel *et al.*, 2006) and from remote sensing data (Stöckli & Vidale, 2004; Julien & Sobrino, 2009; Hamunyela *et al.*, 2013). However, the reported trends in Growing Season Length (GSL) vary considerably, depending on the methodology used, the temporal and spatial extent and the data resolution. Moreover, most studies have focused on an advancement of spring events (through green-up and Start-Of-Season, SOS) and only few have tested for a climatically induced prolongation (or advancement) of the End-Of-Season (EOS) (Jeong *et al.*, 2011; Høgda *et al.*, 2013). The timing and rate of autumn senescence have been found to vary across the canopy even more than those of spring development (Richardson *et al.*, 2009), making this process potentially harder to track than green-up. Here, we provide a comprehensive LSP analysis over all of Europe by assessing long-term trends in LSP metrics. We put focus on the relative contribution of SOS and EOS dynamics, since both may have different ecological implications and a different set of underlying drivers.

Given the temperature increases that have shaped the last three decades, we hypothesize that growth constraints have generally eased in Europe over the past 30 years, resulting in longer GSL. Going into more detail and towards attribution of these changes, our second hypothesis is that GSL trends varied between Europe's heterogeneous ecological zones and between spring and autumn, because of differing controlling factors to vegetation dynamics as well as the variety of human pressures in Europe.

Material and methods

In our approach, we extracted LSP metrics (i.e. SOS, EOS and GSL) from the longest continuous NDVI record available to date, and analysed the spatial and temporal variation in these LSP metrics per landscape unit. The time series were smoothed to remove biased observations and LSP metrics were extracted using a maximum-increase and a midpoint method. The LSP metrics were used to detect change and spring–autumn symmetry.

Time series of vegetation activity

We used the newest release of the Advanced Very High Resolution Radiometer (AVHRR) NDVI, which is the nonstationary NDVI version 3 dataset made available by NASA's Global Inventory Monitoring and Modelling Systems (GIMMS) group (Pinzon *et al.*, 2004; Tucker *et al.*, 2005; Pinzon & Tucker, 2014). This dataset is more commonly referred to as $NDVI_{3g}$, with the suffix 3g referring to the 3rd generation processing applied to correct for orbital drift effects, calibration, viewing geometry, stratospheric volcanic aerosols and other errors unrelated to vegetation change (Pinzon *et al.*, 2004; Tucker *et al.*, 2005; Sobrino *et al.*, 2008). $NDVI_{3g}$ contains global NDVI observations at ca. 8 km spatial resolution, derived from AVHRR channels 1 and 2 – corresponding to red (0.58 – 0.68 μm) and infrared wavelengths (0.73 – 1.1 μm), respectively. The dataset spans from July 1981 to December 2011 and has a bimonthly temporal resolution. Each 15-day data value is the result of Maximum Value Compositing (MVC) (Holben,

1986), a process aiming to minimize the influence of atmospheric contamination (e.g., from aerosols and clouds). This technique assumes that NDVI undergoes smooth variations throughout the year (Sellers *et al.*, 1996) and that atmospheric disturbance is responsible for sharp temporary drops in values, creating time series outliers (Holben, 1986). We extracted data for all European land pixels from all complete years of GIMMS NDVI$_{3g}$ (i.e. 1982–2011), and stacked them by calendar year (January–December).

European Landscape classification

The latest version (v3) of LANMAP (Mücher *et al.*, 2010) was used to classify landscapes for the LSP analysis. This classification is available at a scale of ~1:2M and covers all of Europe: it extends from west to east covering the area between the Atlantic coast and the Ural Mountains. More precisely, the region stretches from Iceland (NW) to Nova Zembla (NE) and from Gibraltar (SW) to Azerbaijan (SE). This area covers about 11 million km^2 and represents around 220 000 NDVI$_{3g}$ pixels. Four key types of data were used to delineate landscape units: climate, altitude, parent material (geological information) and land cover/land use. The resulting hierarchical map includes four levels from the highest (Level 1) dividing Pan-Europe into eight climatic zones to the lowest (Level 4) dividing Europe into 350 landscape classes (Mücher *et al.*, 2010). Within LANMAP, landscapes are defined as 'ecological meaningful units where many processes and components interact' (Mücher *et al.*, 2010). This classification therefore creates a more ecologically significant stratification than would land use/land cover alone. Also, the use of a landscape classification as opposed to more 'conventional' land cover classifications (such as GLC2000, GLOBCOVER or similar) is in line with European environmental reporting efforts. An illustration of LANMAP is presented in Figure S1 in Data S1 (Supporting Information section).

The LANMAP classification system was reprojected and rasterized, using a centre-pixel approach, to match the 8-km grid of the NDVI$_{3g}$ dataset. Binary masks were created for Level 1 and Level 4 classes (climatic zones and landscape classes, respectively). After extracting LSP metrics on a pixel-by-pixel basis for the whole region, these LANMAP classes were used to aggregate pixels into ecologically meaningful classes, and thus better interpret results.

Harmonic analysis

We used harmonic analysis to model yearly NDVI profiles as smooth curves, which can be used for extracting of phenological metrics. The Harmonic Analysis of NDVI Time Series (HANTS) algorithm (version 1.3, Fast Fourier implementation) (Roerink *et al.*, 2000, 2003; de Wit & Su, 2005) has been shown to effectively represent the intra-annual variability of GIMMS NDVI data, particularly in regions outside the tropics and the high latitudes (de Jong *et al.*, 2011). HANTS describes the seasonal pattern in NDVI through low-frequency sine functions, which can be used to analytically derive LSP metrics.

A variety of smoothing algorithms have been used in the field of LSP (see for instance [(de Beurs & Henebry, 2010) for a review] but there is no consistently superior performing method for global applications (Reed *et al.*, 2003; Atkinson *et al.*, 2012). We choose HANTS based on its capacity to analytically represent the growing season and to be widely applicable for the extraction of phenological metrics (White *et al.*, 2009). A detailed description of the HANTS parameterization is given in the Table S1.

### Deriving the LSP indices: SOS, EOS and GSL

Our choice of two LSP indicators was based on the comprehensive study of White *et al.* (2009), acknowledging the wide variety of LSP metrics described in the literature (Reed *et al.*, 1994, 2003; White *et al.*, 2009; de Beurs & Henebry, 2010). In their intercomparison and validation of 10 NDVI-derived Start-Of-Season (SOS) metrics, White *et al.* demonstrated a strong variability of average SOS date estimates, reaching differences as high as ± 60 days between individual methods. However, they also put forward two indicators – Midpoint$_{pixel}$ and Max-increase (corresponding to HANTS-FFT in their study) – as best matches to both measured and modelled phenological observations. We therefore considered these two as the most appropriate for use in our study, and refer to them as MP (Midpoint$_{pixel}$) and MI (Max-increase).

We interpolated the HANTS-smoothed NDVI$_{3g}$ to a daily frequency, using a spline function (Forsythe *et al.*, 1977). Then we used both LSP derivation methods to extract SOS for each NDVI annual profile. MP is a local threshold method, whereby the SOS is defined as the day-of-year at which the NDVI reaches half its annual amplitude. For its implementation, we first translated each pixel's annual NDVI profile to a ratio, based on its annual range [Eqn (1)]:

$$\text{NDVI}_{\text{ratio}} = \frac{\text{NDVI} - \text{NDVI}_{\min}}{\text{NDVI}_{\max} - \text{NDVI}_{\min}} \qquad (1)$$

We then extracted each SOS as the first day of year at which NDVI$_{\text{ratio}}$ is greater than the midpoint, i.e. when NDVI$_{\text{ratio}} > 0.5$, as shown in Fig. 1a. The MI algorithm, on the other hand, defines SOS as the date of maximum increase in NDVI i.e. as the maximum of the first derivative, located between the maximum annual NDVI value and its first preceding inflection point (Fig. 1b). The EOS, for both methods, is defined as the first day (after SOS) with an NDVI value lower than or equal to the NDVI value at SOS for that given year. SOS and EOS are always expressed in Day-Of-Year (DOY), and the Growing Season Length (GSL) was then calculated as the number of days between SOS and EOS.

For some pixels, the growing season may straddle the end of the calendar year. This is common in southern Europe, where the growing season may occur during winter. Deriving LSP metrics from such profiles necessitated a specific approach, since both MP and MI algorithms were constrained to the calendar year. We thus identified all pixels for which the SOS date was found to be within the first GIMMS scene of the calendar year. For each of these cases, the NDVI profile for
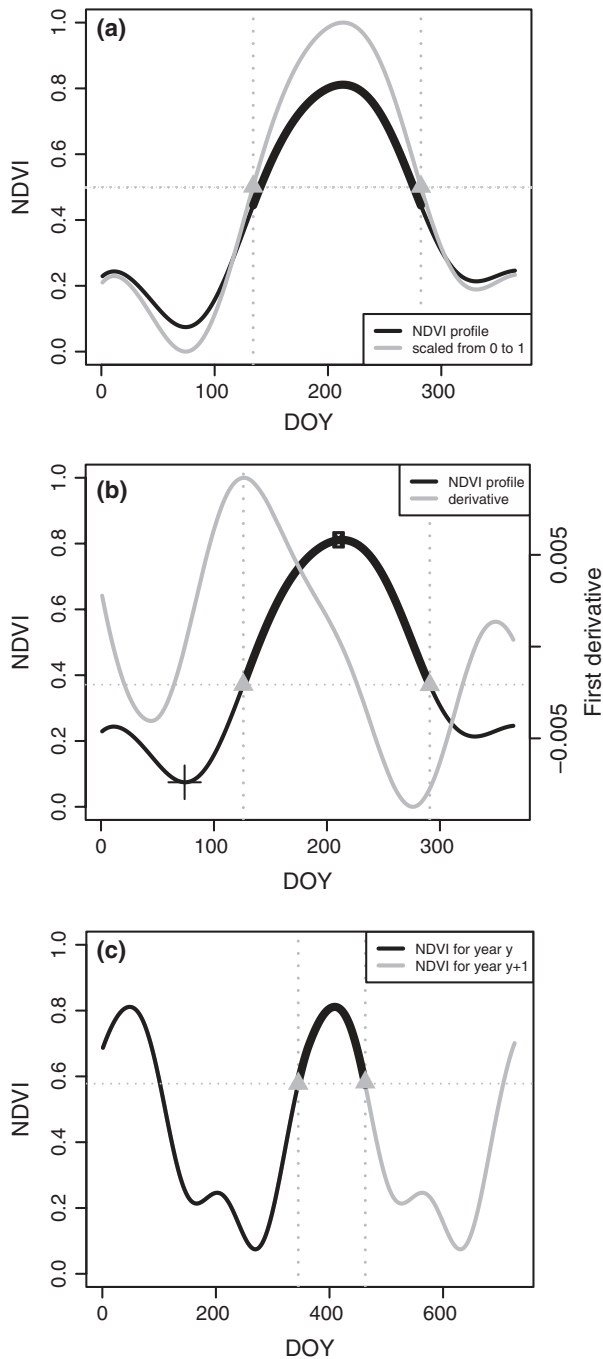
Fig. 1 Illustration of midpoint$_{pixel}$ (MP) (a) and max-increase (MI) (b) methods, as well as a case of growing season straddling two calendar years (c). The black bold line highlights the growing season as extracted from our algorithm. The grey triangles represent start-of-season (SOS) and end of season (EOS) dates, respectively. In (b), the black square refers to the normalized difference vegetation index (NDVI) annual maximum, and the cross refers to the first inflection point preceding SOS.

the following year was appended to the time series (as shown in Fig. 1c), and both LSP metric retrieval algorithms were repeated.

Two types of 'irregular' profiles were considered potentially unstable in our method, and were therefore discarded from our analysis: firstly, pixels for which there is no distinct seasonality (e.g., in arid areas); secondly, pixels with double (or more) growing seasons. The first type was defined as pixels for which the annual NDVI range is lower or equal to 0.1 for more than 10 (of the 30) years. The latter were identified using a flagging algorithm that scanned the distribution of consecutive DOYs considered within the growing season (presented in Figure S2 in Data S1).

Quantification of change and trend symmetry

Linear regression analysis was used to detect trends in LSP metrics. We quantified trends using the slope of the regression line representing the LSP variation over time. The fitted slopes were tested for significance using analysis of variance (ANOVA) with a significance level (α) of 0.05. The Coefficient of Variation (CV) was calculated across years for each pixel and then averaged by landscape class, as a measure of inter-annual variation in GSL. Only pixels for which trends significantly differed from zero were considered in our results. All LSP metrics were derived and analysed for trends using the statistics software R (http://www.r-project.org/, version 3.0.1.).

To quantify the relative contribution of trends in SOS and EOS to the overall GSL changes observed, we calculated the C-index as follows:

$$C = -1 + \frac{2 * abs(\Delta_{SOS})}{abs(\Delta_{SOS}) + abs(\Delta_{EOS})} \quad (2)$$

for which Δ_{SOS} and Δ_{EOS} are the rate of change of SOS and EOS (respectively) and are expressed in days decade^{-1}. The C-index has no unit and varies from -1 to 1. A negative C value means that the change in GSL is mostly attributable to a shift in EOS, whereas a C value close to 1 means that SOS shifts dominate in the overall GSL change. In this respect, we evaluate the symmetry of EOS and SOS shifts over the time period. Figure 2 below illustrates examples of symmetric and asymmetric trends using, as an example, the case of both EOS and SOS contributing to an overall lengthening of the growing season.

Results

The LSP extraction method was successful for 97% of the total number of pixels; the remaining 3% – amounting to around 16 000 pixels – were discarded because of their low annual NDVI range (about 8000 pixels) or the presence of multiple growing seasons during a calendar year (8000 additional pixels). The latter were mostly located in the Mediterranean zone (as illustrated in Figure S3 in Data S1), covering over 31% of its total extent.

Characterization of Pan-European LSP using 30 years of NDVI data

Figure 3 presents the average phenological profiles with their average SOS and EOS dates for the eight
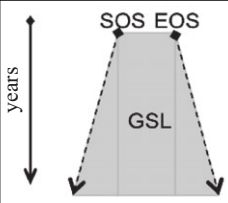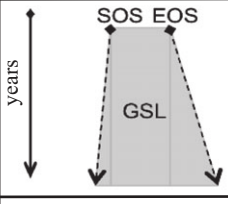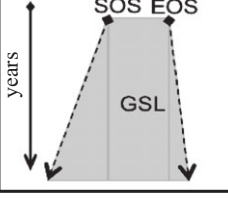
Example	Illustration	C-value	Symmetric trends
1)	SOS EOS / years / GSL	C = 0	Yes
2)	SOS EOS / years / GSL	C < 0	No
3)	SOS EOS / years / GSL	C > 0	No

Fig. 2 Symmetry in trends and corresponding C values.

Pan-European climatic zones. The Boreal and Alpine zones have the highest seasonal variation in NDVI, with differences between winter and summer NDVI greater than 0.6 points. The Mediterranean zone, on the other hand, has the smallest NDVI range, of only approximately 0.15 NDVI points. The Alpine, Boreal, Arctic and but also the Steppic and Anatolian zones are all characterized by very low winter NDVI values ($NDVI_{winter} \leq 0.2$), whereas profiles for the Continental, Atlantic and Mediterranean zones are higher through the whole year. The intra-annual NDVI profiles for the Arctic, Alpine and Boreal zones present a shape that is rather symmetrical around the annual maximum, whereas the others (namely the Anatolian, Steppic and Continental zones) have a slower autumn decline than spring increase in NDVI (Fig. 3).

Figure 4 illustrates differences in SOS, EOS and GSL between climatic zones and between the two methods used to derive LSP indices. There was generally good agreement between the methods regarding average and relative GSL values for most climatic zones. However, the MI method led to consistently smaller estimates of GSL than the MP method. Generally, EOS values varied more between the two methods than did SOS values, which were relatively stable between the two methods for all climatic zones. The highest average GSL values were found for the Atlantic and Continental zones and the lowest are for the Arctic and Anatolian zones. Over the whole 30 year period, the average GSL in Pan-Europe is approximately 159 ± 30 days i.e. about 5.5 months.

Figure 5 presents the average GSL and its CV for each landscape class (LANMAP Level 4). GSL declined with latitude from >180 days in southern and central Europe to <120 days in northern Europe. Both LSP derivation methods yielded the highest average GLS values in Germany, France, the Balkans and the United Kingdom. Values derived by the MI method had a higher CV in most areas but the largest CVs were found by both methods in the Mediterranean and Atlantic zones and in the west of the Caspian Sea (Fig. 5b). These high CV are linked to particularly high interannual variability in GSL in these areas rather than to high spatial variability in GSL within climatic zones or geographic areas.

Interannual trends in Growing Season Length

We found significant trends (α = 0.05) in NDVI3 g-derived GSL over 18–30% of the Pan-European region (Table 1). Consistent with our first hypothesis, both LSP derivation methods revealed an average GSL increase for the Continental, Boreal and Alpine zones (Fig. 6). In particular, significant trends covered up to 46% and 32% of the total area of the Boreal and Continental climatic zones, respectively. For the whole of Europe, an average lengthening between 18–24 days per decade was recorded (MI method for the first, MP for the latter estimate). However, in contrast with our first hypothesis, significant GSL decreases over the past 30 years occurred in the Steppic and Atlantic climatic zones. For the Mediterranean and Anatolian zones, the two derivation methods yielded opposite interannual trends indicating inconsistent temporal trends in GSL over the 30-year observation period. These were also zones for which most pixels had to be either discarded or did not show a significant linear trend over the years: only about 14–17% pixels in the Anatolian and about 7–11% in the Mediterranean zones showed significant linear trends (Table 1).

Although the Boreal and Continental climatic zones showed a relatively uniform increase in GSL over the 30-years observation period (Fig. 7a), considerable within-zone variation was found across most of Pan-Europe. The variation between landscape classes was greatest in the Atlantic, Mediterranean and Steppic climatic zones (Fig. 7a). Looking at the spatial distribution of the significant trends that are responsible for the above-described average trends, we see that positive changes were concentrated in Southern Fennoscandia, in Western Russia, and in pockets of continental Europe (Fig. 7b). Negative changes, on the other hand, were mostly concentrated in Western France, the Po valley in Italy and around the Caspian Sea. Among all the significant trends found (covering 18–30% of the study area
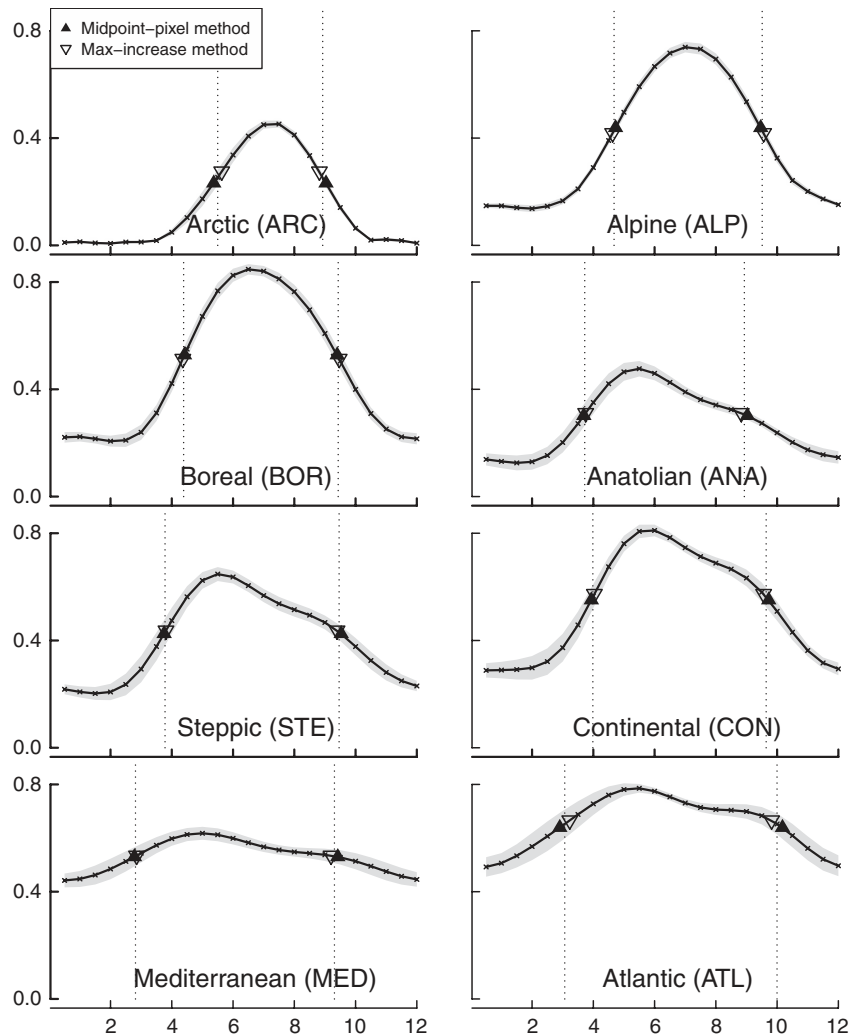
Fig. 3 Normalized difference vegetation index (NDVI) average annual profile, with start-of-season (SOS) and end of season (EOS) for the eight LANMAP-derived climatic zones of Europe. The time series (solid lines and crosses) are plotted with their standard deviations (shaded). SOS and EOS are solid and empty triangles as derived by the midpoint$_{pixel}$ (MP) or max-increase (MI) methods, respectively.

depending on the LSP metric used), 69–85% were positive (for MI and MP methods, respectively). This means that 12–24% of the land surface area of Europe was characterized by increasing GSL from 1982–2011 whereas only 4–5% by decreasing GSL.

Increases in GSL decline across Europe from the west to the east (Fig. 8a) and are largest in mid-latitudes (Fig. 8b). For the latter the MI method yielded more scattered values than did the MP method, reflecting the higher variability of results using the first of the two methods.

Trends in green-up and senescence dates

Figure 9 shows the intra- and interannual variations in the NDVI$_{3g}$ data. For Europe in general (Fig. 9a) the

two methods to derive LSP indicators give very similar results although the SOS dates are consistently earlier with the MP than with the MI method. In the regional plots (Fig. 9b), the contour lines indicate the high inter-annual variability in NDVI values for the Mediterranean, Anatolian, Steppic and Atlantic zones. Figure 9 and Table 2 also provide information on the attribution of a general GSL trend to changes in SOS, EOS or both. For three zones in particular, the C-Index values are negative, indicating that EOS trends tend to be greater than SOS ones: these are the Continental, Mediterranean and Steppic zones. Also, EOS trends are more often significant than SOS ones (Table 2), as seen for the Anatolian, Atlantic and Steppic zones. More precisely, the strongest absolute values of the C-index are found in regions with an overall shortening growing
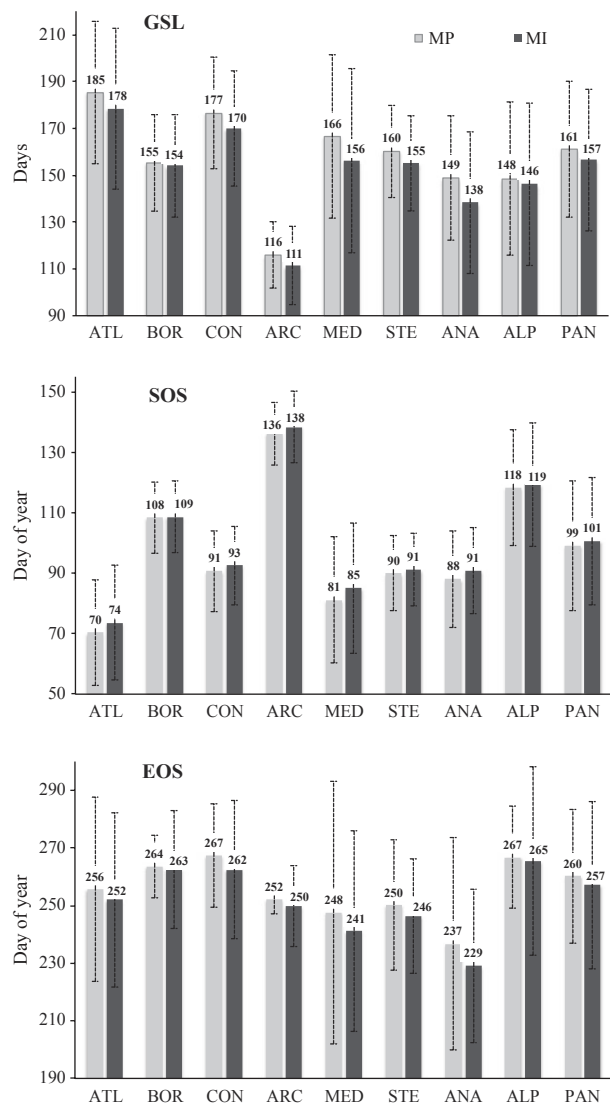
Fig. 4 Average growing season length (GSL) (top, in days), start-of-season (SOS) and end of season (EOS) (middle and bottom, in day-of-year) from 1982–2011 in eight climatic zones (LANMAP Level 1) and for all of Europe (PAN) derived by midpoint_pixel (MP) and max-increase (MI) methods. MP results are in light grey, MI in dark grey.

season, namely the Steppic and Mediterranean zones. In all other zones, C-values are close to 0 or differing in sign depending on method; indicating an approximately equal contribution of SOS and EOS to the overall growing season trend identified.

Discussion

After comparing results as derived from MP and MI methods, a number of conclusions on Pan-European LSP and on the trends over the past 30 years can be drawn, as discussed in detail below.

LSP metrics comparison

Based on the findings of White *et al.* (2009), some level of difference between LSP indicators was anticipated, and should be acknowledged. Firstly, for most climatic zones the MI method gives a later SOS date than MP (Figs 3 and 5). This was expected, since White *et al.* (2009) found MI to be 'consistently late in SOS estimation'. Secondly, the MI method shows a larger year-to-year variation in SOS, and thus in EOS, estimates (Fig. 5b). The conservative (i.e. late) SOS date estimates result in a reduced range of variation and small variations are thus easily over-emphasized. Also, by focusing on the slope of the NDVI profile, the MI method is more prone to variations in seasonal shape, compared to MP, thus leading to fewer pixels displaying significant trends (Table 1). Thirdly, Southern landscapes show the greatest divergence in average GSL between methods (Fig. 4), and these latitudes (albeit for North America) were already identified as areas of high variability between LSP metrics (White *et al.*, 2009). They highlighted the Mediterranean climatic zone of North America as the one where the ability of satellite methods to retrieve SOS is lowest. This is confirmed in our European study, where we find that this zone has the highest between method variability, both in terms of average GSL and the trends found, as well as highest interannual variation in derived GSL (highest CV in Fig. 5) and lowest NDVI annual range (Fig. 3). For this climatic zone, it is important to bear in mind that over 7000 pixels (i.e. more than 31% of the zone) were discarded based on the presence of two (or more) growing seasons within a single year. As shown in Figure S3 in Data S1, excluded pixels covered large parts of Spain and Portugal. There the LSP characteristics are only partly representative of the Mediterranean zone, and particular caution must be used in their interpretation.

Despite these differences, the MP and MI methods show a generally good agreement in both the type and the magnitude of LSP changes observed (Fig. 7 and Figure S4 in Data S1). Although the overall number of pixels with significant trends is much lower for the MI method (Table 1), the distribution of the trends and the relative LSP average change per climatic zone are very similar between the two methods (Fig. 7 and Figure S4 in Data S1). This provides further confidence in the trends derived, and which we discuss hereafter.

LANMAP-dependent growing season trends

In our results, 18–30% of the total study area displayed statistically significant change in GSL. When only significant trends were considered, over 60% demonstrated a lengthening of the growing season. As
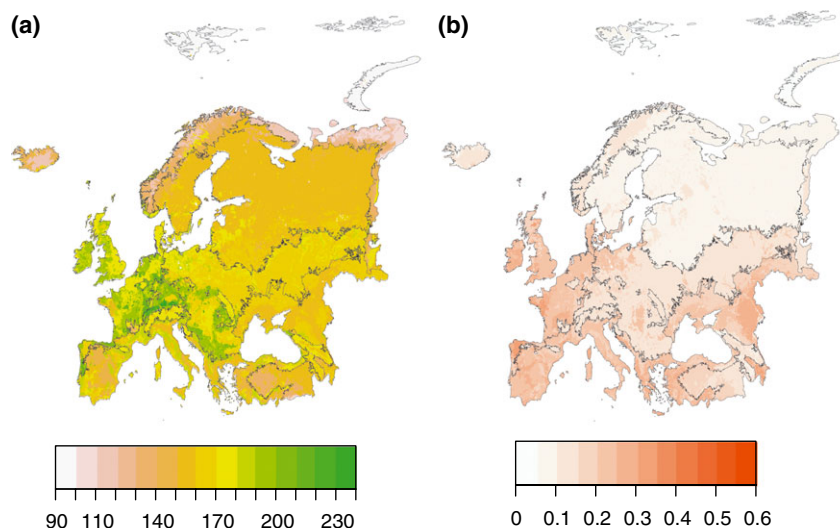
Fig. 5 Mean growing season length (GSL) (a, in days) and coefficient of variation (CV) (b, no unit) by landscape class, as derived from midpoint_pixel (MP). LANMAP Level 1 zones borders are drawn in black. The corresponding figure for max-increase (MI) is in the Supporting Information section (Figure S4 in Data S1).

**Table 1** Percentage of significant trends found in each LAN-MAP Level 1 zone

	% of pixels with significant GSL change	
Climatic zone	MP	MI
Atlantic	18	12
Boreal	46	26
Continental	32	16
Arctic	5	4
Mediterranean	11	7
Steppic	17	19
Anatolian	17	14
Alpine	16	12
Pan-Europe	30	18

hypothesized, we found an average lengthening of the growing season in Europe of 18–24 days decade^{-1} for 1982–2011. These results appear to be consistent with previous studies based on ground observations (Menzel & Fabian, 1999; Ciais et al., 2008) and remote sensing data (Stöckli & Vidale, 2004; Jeong et al., 2011; Eastman et al., 2013). Stöckli & Vidale (2004) found an average lengthening of 9.6 days decade^{-1} for the a narrower 'European domain' for 1982–2001; (Julien et al., 2006) highlighted Scandinavia and Western Russia as areas with significant increase in NDVI amplitude in the period 1982–1999; and a study focusing on Fennoscandia concluded that Southern areas present the greatest SOS advance of the area (Høgda et al., 2013). However, it is important to note that our areas of

strongest growing season lengthening do not correspond to the areas highlighted by Eastman et al. (2013), who also used NDVI$_{3g}$. This may be explained by the fact that these zones are particularly high Leaf Area Index (LAI) areas, where – despite a significantly longer growing season – NDVI may saturate and therefore not increase the annual amplitude sought by Eastman et al. in their analysis of Fourier components.

The trends observed are spatially variable and differ considerably between both climatic zones and landscape classes, and are therefore in agreement with our second hypothesis. The Boreal and Continental climatic zones appear to have undergone the greatest average lengthening of the growing season in the last 30 years. In these zones, vegetation growth is mainly limited by photoperiod and temperature (Nemani et al., 2003). Various studies have reported shifts towards more favourable conditions for plant growth particularly in boreal regions, for instance by a decline in snow cover duration in the boreal forest (Goetz et al., 2005; Eastman et al., 2013), or through a 50% increase in seasonal amplitude of CO_2 observations at high latitudes since 1960 (Graven et al., 2013). More favourable conditions may lead to an expanded growing season, meaning a longer carbon uptake period (Metzger et al., 2008), and increased biomass formation. This was put forward by (Menzel & Fabian, 1999), who observed a European growing season lengthening of 10.8 days from 1960–1990s, based on ground phenological observations. These areas of lengthening are mostly concentrated in Southern Fennoscandia, Western Russia and within pockets of continental Europe.
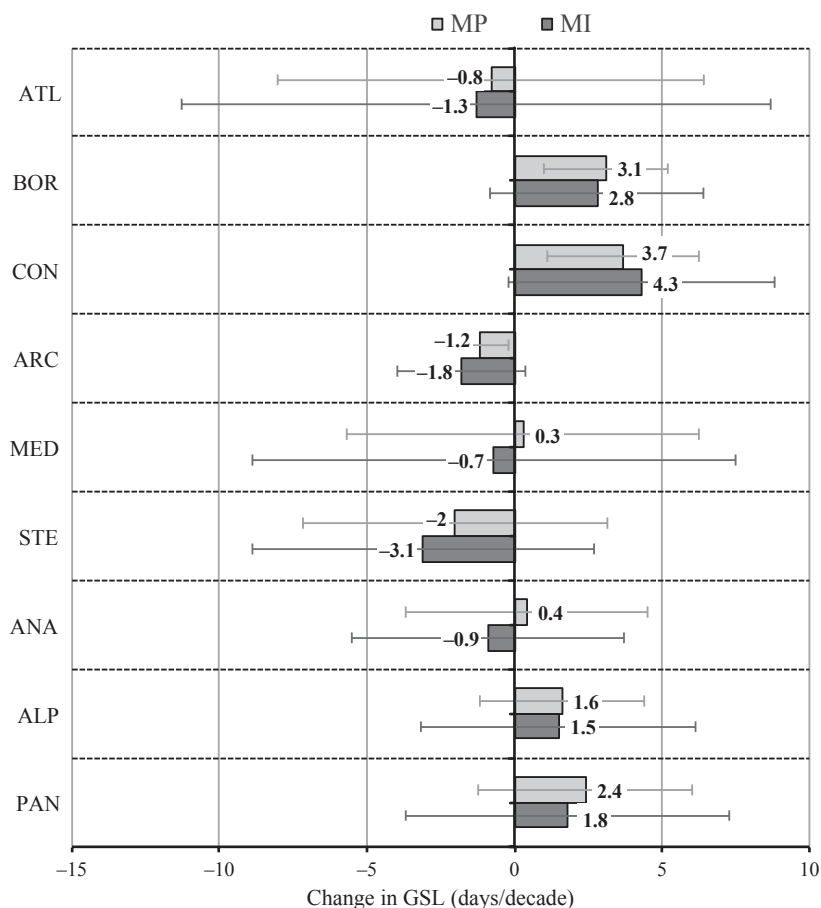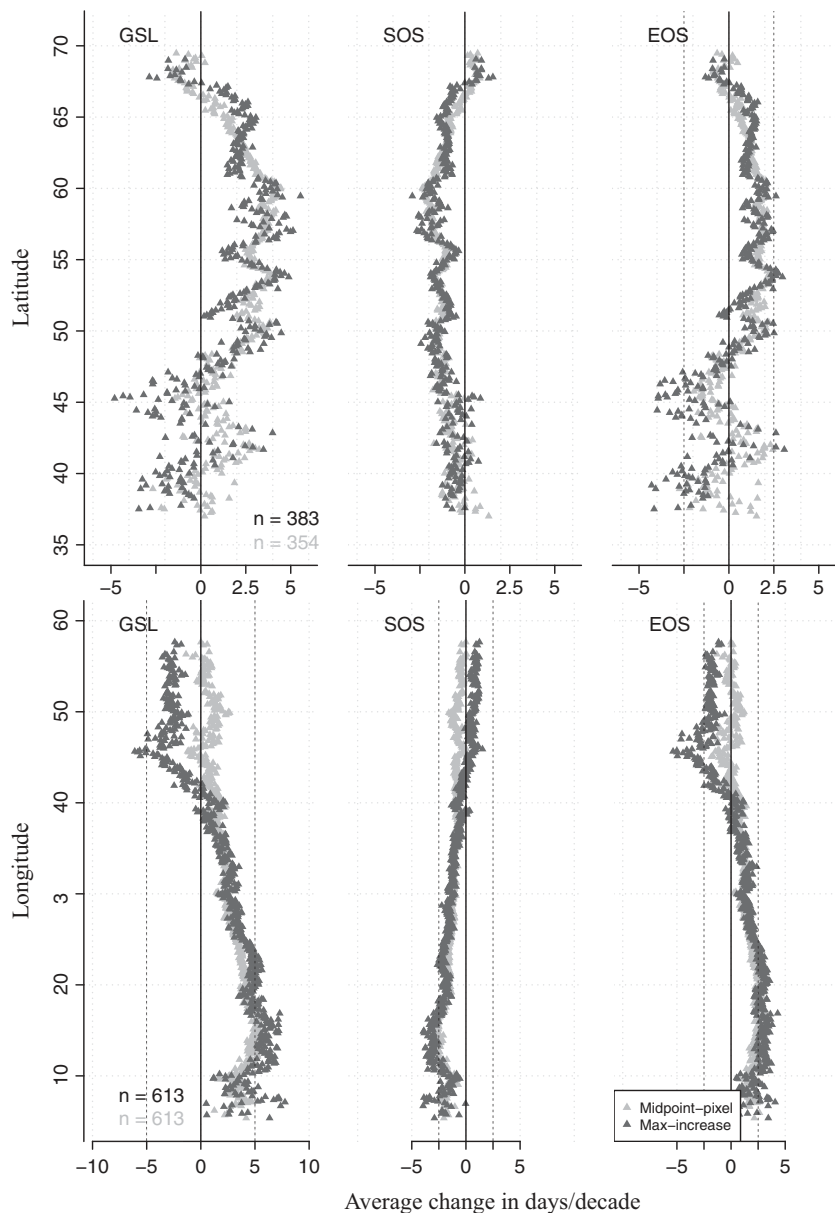
Fig. 6 Average growing season length (GSL) change (in days decade^{-1}) and its standard deviation (error bars) for each climatic zone. Only pixels with trends significant at 5% were considered.
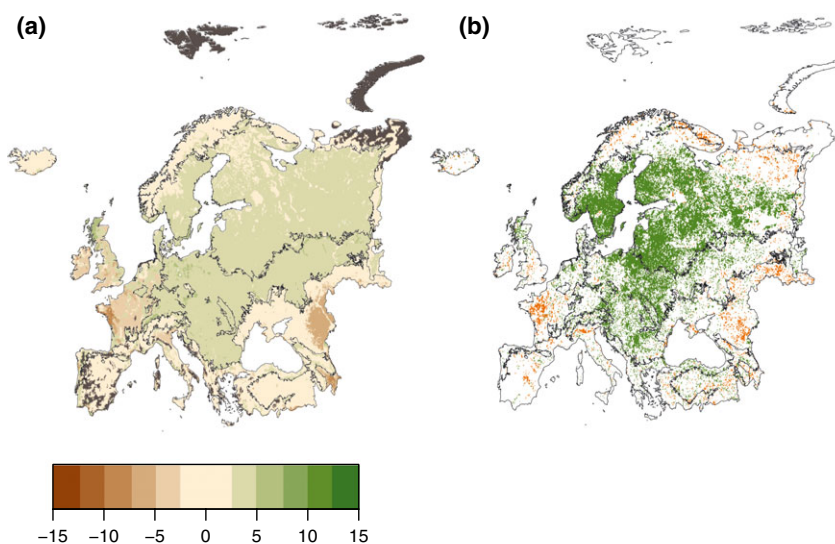
Fig. 7 Average interannual linear trends in growing season length (GSL) (in days decade^{-1}) using the midpoint$_{pixel}$ (MP) method, averaged by landscape class (a) and on a per-pixel basis (b). In (b), pixels with overall lengthening of the growing season are represented in green, pixels with overall shortening of the growing season are in orange. The corresponding figure as derived by the max-increase (MI) method is presented in the Supporting Information section (Figure S5 in Data S1).

Fig. 8 Variation in interannual change (days decade^{-1}) in growing season length (GSL), start-of-season (SOS) and end of season (EOS) across latitude (top) and longitude (bottom) in Europe. Light and dark light grey colours represent results using the midpoint$_{pixel}$ (MP) and max-increase (MI) methods, respectively.

Relating to our second hypothesis, it should be noted that some areas within Pan-Europe show considerable decrease in GSL. Areas of shortening of the growing season are concentrated in Western France, the Po region in Italy and around the Caspian Sea. An average shortening of the growing season is also present over 4–5% of the Arctic zone. However, this region being

most prone to HANTS-induced artefacts (de Jong *et al.*, 2011), we do not discuss it here. The Mediterranean and Anatolian zones show unclear patterns – with results being strongly dependent on the method used. Southern Europe – where seasonal changes in moisture availability limit vegetation activity – is believed to be shifting towards increasingly arid and warm conditions

Fig. 9 Interannual and seasonal variability in Normalized difference vegetation index (NDVI) (a) for Pan-Europe, and (b) for each climatic zone individually. Blue and red markers indicate start-of-season (SOS) and end of season (EOS) as derived from the midpoint$_{pixel}$ (MP) and max-increase (MI) methods, respectively. Solid lines represent trends significant at 5% level whereas dashed lines are not significant.

(a)

(b)
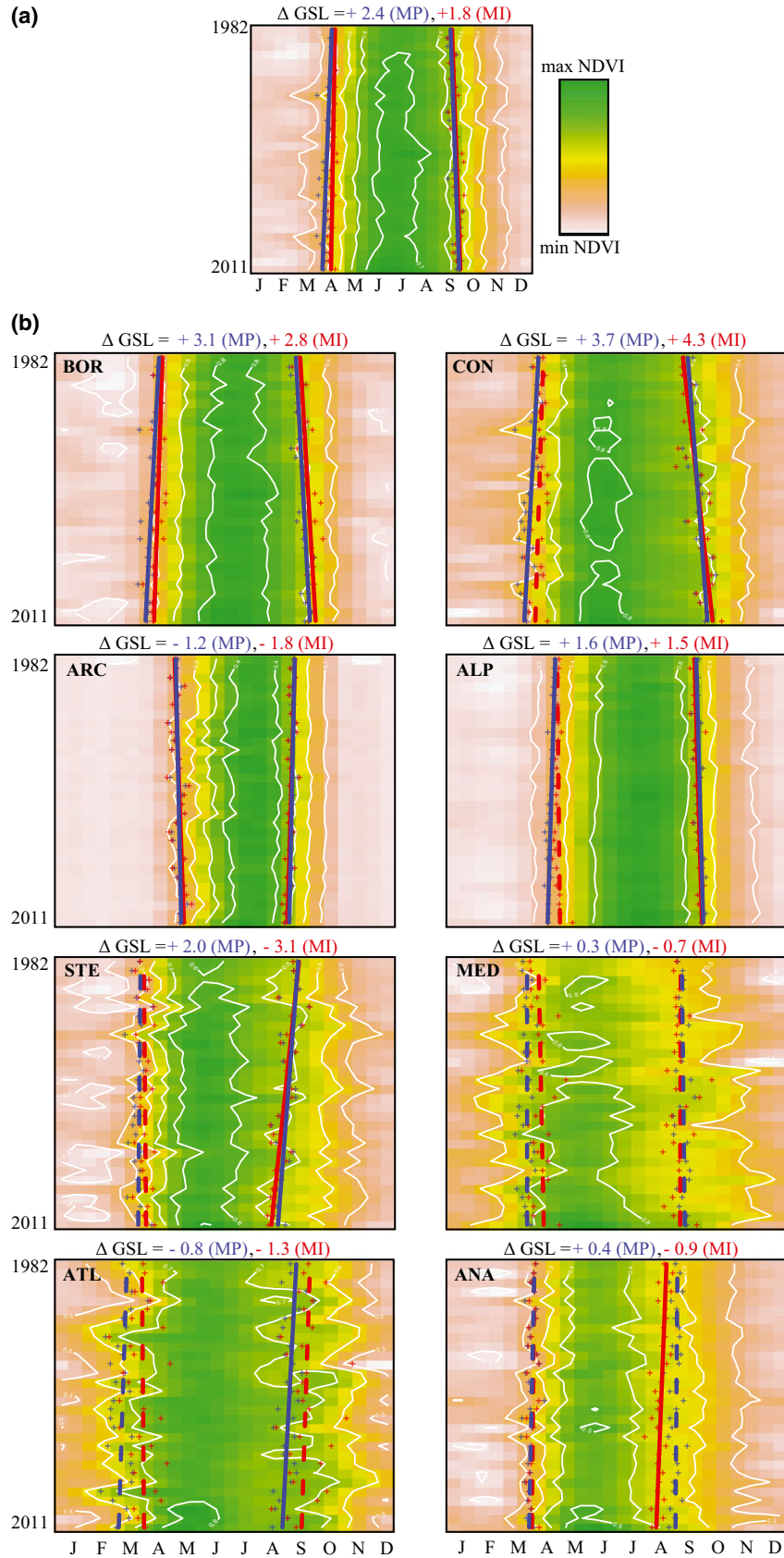
(Julien *et al.*, 2006). Moreover climate change models have indicated that the summer drought that is characteristic of Mediterranean ecosystems is likely to increase in duration and intensity with intensifying climate change (IPCC, 2007; Richardson *et al.*, 2013). Such a scenario is likely to translate to an earlier onset of spring that is offset by an earlier and longer-lasting summer drought period (decreasing vegetation activity).

With each pixel representing ca. 64 km^2 surface area, most European pixels represent multiple land covers, which complicates the possibility of validating derived LSP metrics with ground phenological data. The latter are mostly species-centric, whereas our LSP data represent multiple land covers in an area-averaged fashion. Moreover, although LSP is related to plant phenology via the absorption and reflectance of photosynthetically active radiation, this parameter also includes the confounding effects of soil, snow and atmosphere (Kathuroju *et al.*, 2007) as well as potential nonclimatic factors influencing the land surface, such as anthropogenic disturbance or fires (White *et al.*, 2009). These render LSP values, particularly at this coarse scale, not directly comparable to field-derived vegetation phenology data (Badeck *et al.*, 2004). Smaller-scale or landcover specific studies have found LSP metrics and ground-observation trends to be comparable [e.g.,(Hamunyela *et al.*, 2013)] but at a Pan-European scale, comparison with field-derived phenological trends using ground data remains difficult.

Disentangling drivers of LSP metric change – which may be either climatic, anthropogenic or both (Evans & Geerken, 2004; Yin *et al.*, 2012; de Jong *et al.*, 2013) – also requires further research. For instance, land abandonment in the post-Communist Eastern Europe has been widely documented in the literature (Kuemmerle *et al.*, 2009), and the Po plain of Italy is known to have undergone rapid socio-economic transformations in the last 30 years (Marchetti, 2002). The Fennoscandian lowlands and southern France are strongly agricultural, and therefore the shortening of the growing season observed may be linked to warming-induced shortening of the growing season (Lobell *et al.*, 2011) as well as to agricultural practices. Indeed, in cultivated areas, earlier harvesting may lead to a shortening trend in our NDVI-derived growing seasons. However, the attribution of trends to their corresponding drivers remains beyond the scope of this article.

Asymmetry in SOS and EOS trends

Our results show an equal or stronger association of the GSL trends with EOS delay/advance, than with SOS ones (Table 2). This asymmetry in SOS vs. EOS trends is an important finding because autumn trends are generally not as well-documented as spring ones in the literature (Jeong *et al.*, 2011; Richardson *et al.*, 2013). In Figs 6 and 9, for example, we see that EOS trends dominate the GSL trends: we generally find 'delayed' autumn for those zones with overall lengthening, and advance in autumn date for those zones with an average shortening of the vegetation period. Also, EOS trends are generally stronger (deviate more from 0) than SOS trends for most climatic zones (Fig. 6). These results highlight the importance of including EOS in LSP studies. Furthermore, two recent LSP studies (one for Northern temperate forests and another focusing on the Appalachian) have concluded that the extended length of season found since 1982 – a process initially attributed mainly to an earlier start-of-season –may have shifted, in recent years, to a considerable delay in end-of-season (Jeong *et al.*, 2011; Zhao *et al.*, 2013).

In Europe, these advanced EOS dates may be simply linked to areas of land use change, or to the increasing importance of limiting factors to plant growth at the end of the season. For instance, one limit could be insufficient water availability at the end of the growing season. These hypotheses remain to be tested in future studies.

Conclusions and outlook

In this landscape-based assessment of LSP trends from 1982 to 2011, the NDVI$_{3g}$ dataset provides us with the opportunity to document intra-annual dynamics of

Table 2 Trends in start of season (SOS) and end of season (EOS) (in days/decade) and C index value for each climatic zone. For all climatic zones, the first row indicates results from the MP method and the second row shows results from MI. Stars indicate statistical significance

Climatic zone	ΔSOS	ΔEOS	C–Index
ATL	−1	−1.8**	−0.3
	−0.8	−2.1	−0.4
BOR	−1.5***	+1.6***	0
	−1.3***	+1.4***	0
CON	−1.6***	+2.2***	−0.2
	−1.9*	+2.4***	−0.1
ARC	+0.6**	−0.6***	0
	+1**	−0.8***	0.1
MED	−0.1	+0.2	−0.3
	−0.2	−0.9	−0.6
STE	−0.4	−2.4***	−0.7
	−0.1	−3.2***	−0.9
ANA	−0.7*	−0.3	0.4
	−0.6	−1.5***	−0.4
ALP	−0.8***	+0.8***	0
	−0.8	+0.7***	−0.1
PAN	−1.3***	+1.1***	0.1
	−1.1**	+0.7***	0.2

European LSP with an unprecedented timespan, adding almost 10 years to the so far longest European LSP study (Stöckli & Vidale, 2004). Despite some marked differences, the two LSP derivation algorithms used gave various consistent results – which we summarize hereafter.

- We observe significant trends in $NDVI_{3g}$-derived growing season length over 18–30% of terrestrial Pan-Europe. These trends vary extensively both within and amongst climatic zones and landscape classes, but overall demonstrate an average lengthening of the growing season in Pan-Europe – which we quantify at 18–24 days per decade on average.
- The Continental and Boreal climatic zones have experienced significant lengthening of the NDVI-derived growing season – with hotspots in southern Fennoscandia, Western Russia and pockets of continental Europe. On the other hand, considerable shortening of the growing season was found in Western France, the Po valley in Italy and around the Caspian Sea. Although associations between these trends and land use/land cover change or shifting environmental conditions are suggested, further study and a finer spatial resolution are needed to discern the drivers of the trends observed.
- Despite more attention having been placed on SOS trends in previous studies, we find equal or stronger contribution of EOS to the overall GSL found throughout Europe. These results highlight the importance for future LSP studies to concentrate just as much on the process of senescence as to annual green-up.

As pointed out in other studies (Atzberger *et al.*, 2013; Zeng *et al.*, 2013), there is a need for cross-sensor intercalibration as a consistency check of the trends found. However, AVHRR has much broader bands than both MODIS and SPOT sensors. This fact, along with the strong differences in both spatial and temporal resolutions, means that we expect sensor choice to have considerable effect on the results found. This is indeed the case in the recent comparison by (Atzberger *et al.*, 2013) who found only moderately good agreement between GIMMS and MODIS over the 2002–2011 period.

Finally, it would be useful to explore the consequences of the observed LSP trends on species distributions at large spatial scales. Indeed, changes in vegetation activity and phenology – as observed from NDVI – can be used to make inferences about habitat conditions, species survival, migration and composition at large scales (Pettorelli *et al.*, 2005; Coops *et al.*, 2013).

Acknowledgements

References

Ahas R, Aasa R, Menzel A, Fedotova VG, Scheifinger H (2002) Changes in European spring phenology. *International Journal of Climatology*, **22**, 1727–1738.

Arora VK, Boer GJ (2005) A parameterization of leaf phenology for the terrestrial ecosystem component of climate models. *Global Change Biology*, **11**, 39–59.

Atkinson PM, Jeganathan C, Dash J, Atzberger C (2012) Inter-comparison of four models for smoothing satellite sensor time-series data to estimate vegetation phenology. *Remote Sensing of Environment*, **123**, 400–417.

Atzberger C, Klisch A, Mattiuzzi M, Vuolo F (2013) Phenological metrics derived over the european continent from NDVI3 g data and MODIS time series. *Remote Sensing*, **6**, 257–284.

Badeck F-W, Bondeau A, Böttcher K, Doktor D, Lucht W, Schaber J, Sitch S (2004) Responses of spring phenology to climate change. *New Phytologist*, **162**, 295–309.

Bailey RG, Ropes L (1998) Ecoregions: the ecosystem geography of the oceans and continents: with 106 illustraions, with 55 in color, Springer.

de Beurs KM, Henebry GM (2005) Land surface phenology and temperature variation in the international geosphere-biosphere program high-latitude transects. *Global Change Biology*, **11**, 779–790.

Ciais P, Schelhaas MJ, Zaehle S et al. (2008) Carbon accumulation in European forests. *Nature Geoscience*, **1**, 425–429.

Coops NC, Schaepman ME, Mücher CA (2013) What multiscale environmental drivers can best be discriminated from a habitat index derived from a remotely sensed vegetation time series? *Landscape Ecology*, **28**, 1529–1543.

de Beurs K, Henebry GM (2010) Spatio-temporal statistical methods for modelling land surface phenology. In: *Phenological Research: Methods for Environmental and Climate Change Analysis*. (eds Hudson IL, Keatley MR) pp. 177–208. Springer, New York.

Eastman J, Sangermano F, Machado E, Rogan J, Anyamba A (2013) Global trends in seasonality of normalized difference vegetation index (NDVI), 1982, Äì2011. *Remote Sensing*, **5**, 4799–4818.

EEA (2012) *Climate Change, Impacts and Vulnerability in Europe: An Indicator-Based Report*. European Environmental Agency, Copenhagen.

Evans J, Geerken R (2004) Discrimination between climate and human-induced dryland degradation. *Journal of Arid Environments*, **57**, 535–554.

Foley JA, Costa MH, Delire C, Ramankutty N, Snyder P (2003) Green surprise? How terrestrial ecosystems could affect earth's climate. *Frontiers in Ecology and the Environment*, **1**, 38–44.

Forsythe GE, Malcolm MA, Moler CB (1977) Computer methods for mathematical computations

Friedl M, Henebry GM, Reed BC et al. (2006) Land surface phenology: a community white paper requested by NASA. Available at: http://cce.nasa.gov/mtg2008_ab_presentations/Phenology_Friedl_whitepaper.pdf (accessed 6 January 2014).

Goetz SJ, Bunn AG, Fiske GJ, Houghton R (2005) Satellite-observed photosynthetic trends across boreal North America associated with climate and fire disturbance. *Proceedings of the National Academy of Sciences of the United States of America*, **102**, 13521–13525.

Graven HD, Keeling RF, Piper SC et al. (2013) Enhanced seasonal exchange of CO2by Northern ecosystems since 1960. *Science*, **341**, 1085–1089.

Hamunyela E, Verbesselt J, Roerink G, Herold M (2013) Trends in spring phenology of western european deciduous forests. *Remote Sensing*, **5**, 6159–6179.

Hazeu GW, Metzger MJ, Mücher CA, Perez-Soba M, Renetzeder C, Andersen E (2011) European environmental stratifications and typologies: an overview. *Agriculture, Ecosystems and Environment*, **142**, 29–39.

Høgda K, Tømmervik H, Karlsen S (2013) Trends in the start of the growing season in Fennoscandia 1982–2011. *Remote Sensing*, **5**, 4304–4318.

Holben BN (1986) Characteristics of maximum-value composite images from temporal AVHRR data. *International Journal of Remote Sensing*, **7**, 1417–1434.

IPCC (2007) Synthesis report. In: *Fourth Assessment Report (AR4) of the Intergovernmental Panel on Climate Change* (eds Pachauri RK, Reisinger A). IPCC, Geneva, Switzerland.

IPCC (2013) *Climate Change 2013: The Physical Science Basis*. In: *Contribution of Working Group I to the Fifth Assessment Report of the Intergovernmental Panel on Climate Change* (eds Stocker TF, Qin D, Plattner G-K, Tignor M, Allen SK, Boschung J, Nauels A, Xia Y, Bex V, Midgley). Cambridge University Press, Cambridge, UK.

Jeong SJ, Ho CH, Gim HJ, Brown ME (2011) Phenology shifts at start vs. end of growing season in temperate vegetation over the Northern Hemisphere for the period 1982–2008. *Global Change Biology*, **17**, 2385–2399.

de Jong R, de Bruin S, de Wit A, Schaepman ME, Dent DL (2011) Analysis of monotonic greening and browning trends from global NDVI time-series. *Remote Sensing of Environment*, **115**, 692–702.

de Jong R, Schaepman ME, Furrer R, de Bruin S, Verburg PH (2013) Spatial relationship between climatologies and changes in global vegetation activity. *Global Change Biology*, **19**, 1953–1964.

Julien Y, Sobrino J (2009) Global land surface phenology trends from GIMMS database. *International Journal of Remote Sensing*, **30**, 3495–3513.

Julien Y, Sobrino JA, Verhoef W (2006) Changes in land surface temperatures and NDVI values over Europe between 1982 and 1999. *Remote Sensing of Environment*, **103**, 43–55.

Kathuroju N, White MA, Symanzik J, Schwartz MD, Powell JA, Nemani RR (2007) On the use of the advanced very high resolution radiometer for development of prognostic land surface phenology models. *Ecological Modelling*, **201**, 144–156.

Kuemmerle T, Chaskovskyy O, Knorn J, Radeloff VC, Kruhlov I, Keeton WS, Hostert P (2009) Forest cover change and illegal logging in the Ukrainian Carpathians in the transition period from 1988 to 2007. *Remote Sensing of Environment*, **113**, 1194–1207.

Lobell DB, Schlenker W, Costa-Roberts J (2011) Climate trends and global crop production since 1980. *Science*, **333**, 616–620.

Marchetti M (2002) Environmental changes in the central Po Plain (Northern Italy) due to fluvial modifications and anthropogenic activities. *Geomorphology*, **44**, 361–373.

Meeus JHA (1995) Pan-European landscapes. *Landscape and Urban Planning*, **31**, 57–79.

Menzel A (2000) Trends in phenological phases in Europe between 1951 and 1996. *International Journal of Biometeorology*, **44**, 76–81.

Menzel A, Fabian P (1999) Growing season extended in Europe. *Nature*, **397**, 659.

Menzel A, Sparks TH, Estrella N *et al.* (2006) European phenological response to climate change matches the warming pattern. *Global Change Biology*, **12**, 1969–1976.

Metzger MJ, Bunce RGH, Jongman RHG, Mücher CA, Watkins JW (2005) A climatic stratification of the environment of Europe. *Global Ecology and Biogeography*, **14**, 549–563.

Metzger MJ, Rounsevell MDA, Acosta-Michlik L, Leemans R, Schröter D (2006) The vulnerability of ecosystem services to land use change. *Agriculture, Ecosystems & Environment*, **114**, 69–85.

Metzger MJ, Bunce RGH, Leemans R, Viner D (2008) Projected environmental shifts under climate change: European trends and regional impacts. *Environmental Conservation*, **35**, 64–75.

Mücher CA, Klijn JA, Wascher DM, Schaminée JHJ (2010) A new european landscape classification (LANMAP): a transparent, flexible and user-oriented methodology to distinguish landscapes. *Ecological Indicators*, **10**, 87–103.

Myneni RB, Keeling C, Tucker C, Asrar G, Nemani R (1997) Increased plant growth in the northern high latitudes from 1981 to 1991. *Nature*, **386**, 698–702.

Nemani RR, Keeling CD, Hashimoto H *et al.* (2003) Climate-driven increases in global terrestrial net primary production from 1982 to 1999. *Science*, **300**, 1560–1563.

Pereira HM, Ferrier S, Walters M *et al.* (2013) Essential biodiversity variables. *Science*, **339**, 277–278.

Pettorelli N, Vik JO, Mysterud A, Gaillard JM, Tucker CJ, Stenseth NC (2005) Using the satellite-derived NDVI to assess ecological responses to environmental change. *Trends in Ecology and Evolution*, **20**, 503–510.

Pinzon J, Tucker CJ (2014) A non-stationary 1982–2012 AVHRR NDVI$_{3g}$ time series. *Remote Sensing*, (Under Review).

Pinzon J, Brown ME, Tucker CJ (2004) Satellite time series correction of orbital drift artifacts using empirical mode decomposition.

Reed BC, Brown JF, Vanderzee D, Loveland TR, Merchant JW, Ohlen DO (1994) Measuring phenological variability from satellite imagery. *Journal of Vegetation Science*, **5**, 703–714.

Reed B, White M, Brown J (2003) Remote sensing phenology. In: *Phenology: An Integrative Environmental Science*, vol. **39** (ed. Schwartz M), pp. 365–381. Springer, the Netherlands.

Richardson AD, Braswell BH, Hollinger DY, Jenkins JP, Ollinger SV (2009) Near-surface remote sensing of spatial and temporal variation in canopy phenology. *Ecological Applications*, **19**, 1417–1428.

Richardson AD, Anderson RS, Arain MA *et al.* (2012) Terrestrial biosphere models need better representation of vegetation phenology: results from the North American carbon program site synthesis. *Global Change Biology*, **18**, 566–584.

Richardson AD, Keenan TF, Migliavacca M, Ryu Y, Sonnentag O, Toomey M (2013) Climate change, phenology, and phenological control of vegetation feedbacks to the climate system. *Agricultural and Forest Meteorology*, **169**, 156–173.

Rockström J, Steffen W, Noone K *et al.* (2009) A safe operating space for humanity. *Nature*, **461**, 472–475.

Roerink G, Menenti M, Verhoef W (2000) Reconstructing cloudfree NDVI composites using Fourier analysis of time series. *International Journal of Remote Sensing*, **21**, 1911–1917.

Roerink G, Menenti M, Soepboer W, Su Z (2003) Assessment of climate impact on vegetation dynamics by using remote sensing. *Physics and Chemistry of the Earth, Parts A/B/C*, **28**, 103–109.

Rouse JW, Haas RH, Deering DW, Schell JA, Harlan JC (1974) Monitoring the vernal advancement and retrogradation (green wave effect) of natural vegetation. pp Page.

Running SW (2012) A measurable planetary boundary for the biosphere. *Science*, **337**, 1458–1459.

Running SW, Nemani RR, Heinsch FA, Zhao M, Reeves M, Hashimoto H (2004) A continuous satellite-derived measure of global terrestrial primary production. *BioScience*, **54**, 547–560.

Sellers PJ, Los SO, Tucker CJ, Justice CO, Dazlich DA, Collatz GJ, Randall DA (1996) A revised land surface parameterization (SiB2) for atmospheric GCMs. part II: the generation of global fields of terrestrial biophysical parameters from satellite data. *Journal of Climate*, **9**, 706–737.

Sobrino JA, Julien Y, Atitar M, Nerry F (2008) NOAA-AVHRR orbital drift correction from solar zenithal angle data. *IEEE Transactions on Geoscience and Remote Sensing*, **46**, 4014–4019.

Stöckli R, Vidale PL (2004) European plant phenology and climate as seen in a 20-year AVHRR land-surface parameter dataset. *International Journal of Remote Sensing*, **25**, 3303–3330.

Tucker CJ (1979) Red and photographic infrared linear combinations for monitoring vegetation. *Remote Sensing of Environment*, **8**, 127–150.

Tucker CJ, Pinzon JE, Brown ME *et al.* (2005) An extended AVHRR 8-km NDVI dataset compatible with MODIS and SPOT vegetation NDVI data. *International Journal of Remote Sensing*, **26**, 4485–4498.

Turner Ii BL, Lambin EF, Reenberg A (2007) The emergence of land change science for global environmental change and sustainability. *Proceedings of the National Academy of Sciences of the United States of America*, **104**, 20666–20671.

White MA, de Beurs KM, Didan K *et al.* (2009) Intercomparison, interpretation, and assessment of spring phenology in North America estimated from remote sensing for 1982–2006. *Global Change Biology*, **15**, 2335–2359.

de Wit AJW, Su B (2005) Deriving phenological indicators from SPOT-VGT data using the HANTS algorithm. In: *Proceedings of the 2nd International VEGETATION user Conference; 1998–2004: 6 years of Operational Activities*. (eds Veroustraete F, Bartholomè E, Verstraeten WW), pp. 195–201. European Commission, Luxembourg.

Yin H, Udelhoven T, Fensholt R, Pflugmacher D, Hostert P (2012) How normalized difference vegetation index (NDVI) trends from advanced very high resolution radiometer (AVHRR) and système probatoire d'observation de la terre vegetation (SPOT VGT) time series differ in agricultural areas: an inner mongolian case study. *Remote Sensing*, **4**, 3364–3389.

Zeng H, Jia G, Forbes BC (2013) Shifts in Arctic phenology in response to climate and anthropogenic factors as detected from multiple satellite time series. *Environmental Research Letters*, **8**, art. no. 035036.

Zhang X, Friedl MA, Schaaf CB *et al.* (2003) Monitoring vegetation phenology using MODIS. *Remote Sensing of Environment*, **84**, 471–475.

Zhao J, Wang Y, Hashimoto H, Melton FS, Hiatt SH, Zhang H, Nemani RR (2013) The variation of land surface phenology from 1982 to 2006 along the appalachian trail. *IEEE Transactions on Geoscience and Remote Sensing*, **51**, 2087–2095.

Zhou L, Tucker C, Kaufmann RK, Slayback D, Shabanov NV, Myneni R (2001) Variations in northern vegetation activity inferred from satellite data of vegetation index during 1981–1999. *Journal of Geophysical Research*, **106**, 20069–20083.

Supporting Information

Additional Supporting Information may be found in the online version of this article:

Data S1. Materials and methods.
Fig S1. The European Landscape Map (LANMAP).
Fig S2. HANTS algorithm description.
Fig S3. Multiple growing seasons mask.
Fig S4. Results from Max-increase method.